

GSA Data Repository 2018027

Tomlinson et al., 2018, An exsolution origin for Archean mantle garnet: *Geology*, <https://doi.org/10.1130/G39680.1>.

ANALYTICAL METHODS

EBSD

Crystallographic orientation of garnet and orthopyroxene in the BP002 megacryst were determined on two near-perpendicular thin sections, which were highly polished and uncoated. Electron back-scatter diffraction (EBSD) patterns were collected using a JEOL 5600 SEM system equipped with a NORD LYS camera (hkl technology) at Geosciences Montpellier. The sample was positioned at a tilt angle 70° from horizontal within the SEM specimen chamber, and was analysed with a 30µm spot at a working distance of 24mm using a 17kV accelerating volt and a beam current of 37nA. Each pattern was indexed against Enstatite Opx AV77 and Pyrope 11 giving Mean Angular Deviations (MADs) of <0.7%. Data was collected using Oxford Instruments Aztec V2.4, and noise reduction was undertaken using HKL Tango using 6 nearest neighbor interpolation. Data processing was done using the MTEX free toolbox for Matlab (version 4.3.2; <http://mtex-toolbox.github.io>).

FGE-SEM-EDS

Major elements were analysed by Field Gun Emission Scanning Electron Microscope Energy Dispersive Spectrometry (FGE-SEM-EDS) at the iCRAG lab at Trinity College Dublin. Analyses was carried out using a Tescan TIGER MIRA3 Variable Pressure Field Emission Scanning Electron Microscope, equipped with two Oxford X-Max 80mm2 detectors, using the Oxford AZtec X-ray microanalysis software. A beam current of ~285pA was used with an accelerating voltage of 20kV. The instrument was calibrated using a suite of appropriate mineral standards from the Smithsonian Institute (Jarosewich et al., 1980). Errors are reported as 2σ. Accuracies of 0.6%, 3.2%, and 1.1% were attained for the natural diopside reference mineral NMNH 117733 for SiO₂, MgO, and CaO respectively. *State-of-the-art field emission gun SEM systems with silicon drift EDX, when operated like electron microprobes, are capable of producing major element data of comparable quality to WDS systems (e.g. Newbury and Richie, 2015).*

LA-ICP-MS

Trace elements were analysed by laser ablation inductively coupled plasma mass spectrometry (LA-ICP-MS) at Trinity College Dublin. The instrument used was a Teledyne Photon Machines Analyte G2 laser ablation system, comprising a 193nm ArF excimer laser and a HeLex II active two-volume ablation cell, coupled to a Thermo iCAPQc ICP-MS. Routine analyses used 2.75Jcm^{-2} an $85\times 85\mu\text{m}$ spot size and a repetition rate of 80Hz for 2400 shots, with each ablation separated by 30s counting on the gas blank. The calibration standard was USGS GSD-1G, and USGS BHVO-2G, USGS GSA-1G and NIST616 were used as quality control standards. Rare earth element (REE) concentrations in orthopyroxene were determined using a $156\times 156\mu\text{m}$ spot size and a repetition rate of 80Hz for 4000 shots and 60s counting on the background, the total sweep time was 5s, following the method of (Stead et al., 2017). Care was taken to clean analyse grain interiors, free from fractures and inclusions. Data reduction was done using Iolite 2.5 using ^{29}Si as the internal standard. Errors are reported as 2σ . Accuracy is typically $<5\%$ for trace elements in USGS reference materials BHVO-G and GS-A.

Jarosewich, E., Nelen, J. A. and Norberg, J. (1980) 'Reference samples for electron microprobe analysis', *Geostandards Newsletter*, 4, pp. 43-47.

Newbury, D. E., and Ritchie, N. W. (2015) 'Performing elemental microanalysis with high accuracy and high precision by scanning electron microscopy/silicon drift detector energy-dispersive X-ray spectrometry (SEM/SDD-EDS)', *Journal of Materials Science*, 50(2), pp. 493-518.

Stead, C. V., Tomlinson, E. L., Kamber, B. S., Babechuk, M. G. and McKenna, C. A. (2017) 'Rare Earth Element Determination in Olivine by Laser Ablation-Quadrupole-ICP-MS: An Analytical Strategy and Applications', *Geostandards and Geoanalytical Research*, 41(2), pp. 197-212.

EBSD RESULTS

Garnet crystals have a fabric, with garnets in both lamellae populations having a dominant crystallographic axis orientation (Fig. 1). The topotactic relationship between the garnet and the host orthopyroxene is not simple, the garnet grains are orientated at an acute angle to orthopyroxene at $(072)_{\text{opx}}//(\text{021})_{\text{grt}}$, $(1351)_{\text{opx}}//(\text{862})_{\text{grt}}$, $(912)_{\text{opx}}//(\text{826})_{\text{grt}}$, $(612)_{\text{opx}}//(\text{627})_{\text{grt}}$, (Fig. 2).

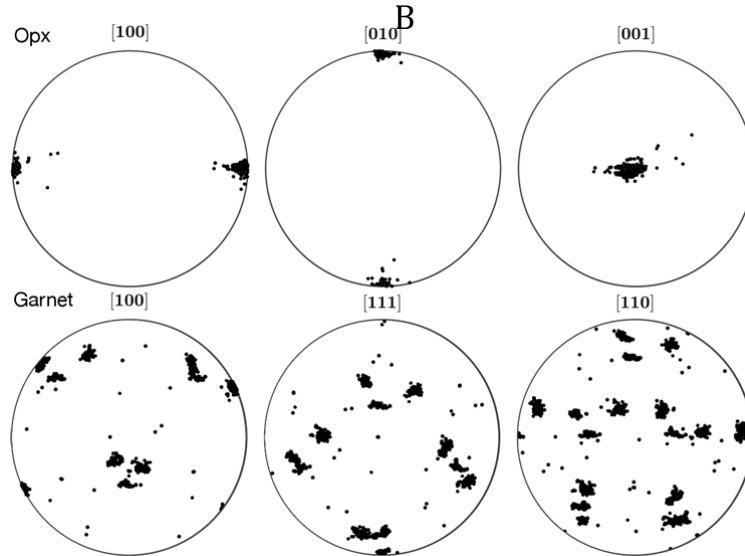


Figure 1: EBSD scatter pole figures showing orientation of different crystallographic axes in the two orthogonal BP002 thin sections (figure 2E and 2F) rotated to look down the pole to the (001) plane of orthopyroxene. Low index surfaces of garnet in different crystals, different lamellae and different lamellae populations are aligned. Note, axes to the {100} (faces), {111}, (space-diagonal planes) and {110} (face-diagonal) planes of the garnet cube.

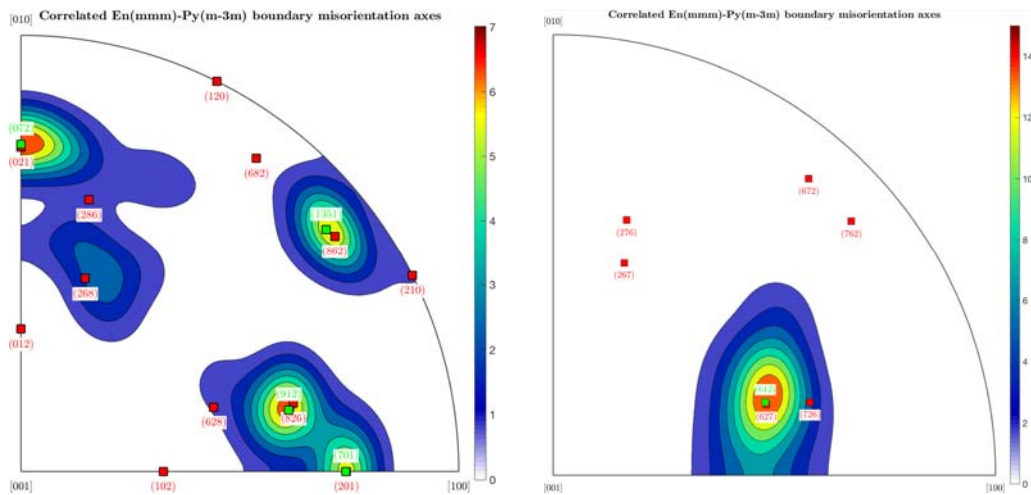


Figure 2: Inverse pole figure showing the orthopyroxene (green) and garnet (red) crystallographic planes corresponding to maxima in the preferred orientation of misorientation axes.

GEOCHEMISTRY RESULTS

Compositional halos around garnet lamellae

Minor compositional zoning is seen around garnet lamellae with Al_2O_3 increasing and SiO_2 decreasing towards garnet lamellae (Fig 1).

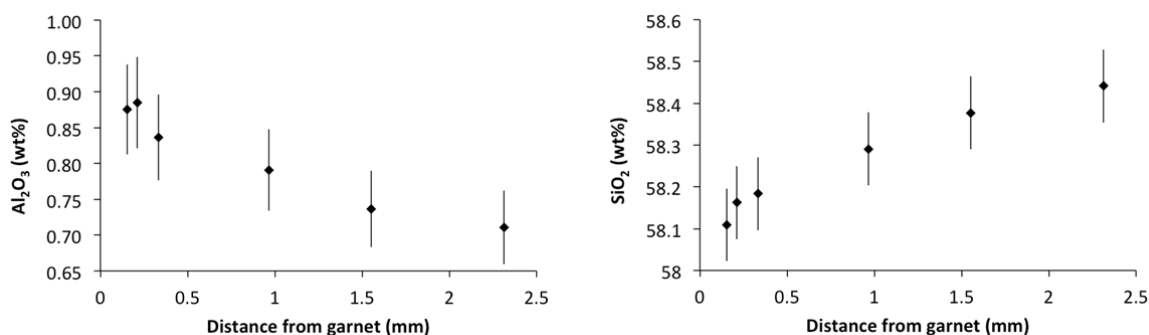


Figure DR1: Gradients in Al_2O_3 and SiO_2 concentration in orthopyroxene around garnet lamellae (Errors are 2σ), data for regions opxrim1 to opxB1 in figure 1.

Trace element equilibration

There is good agreement between the measured garnet/orthopyroxene ratios and those predicted by partition coefficients both for the rare earth elements (Sun and Liang, 2013) and other trace elements (Salters et al, 2002).

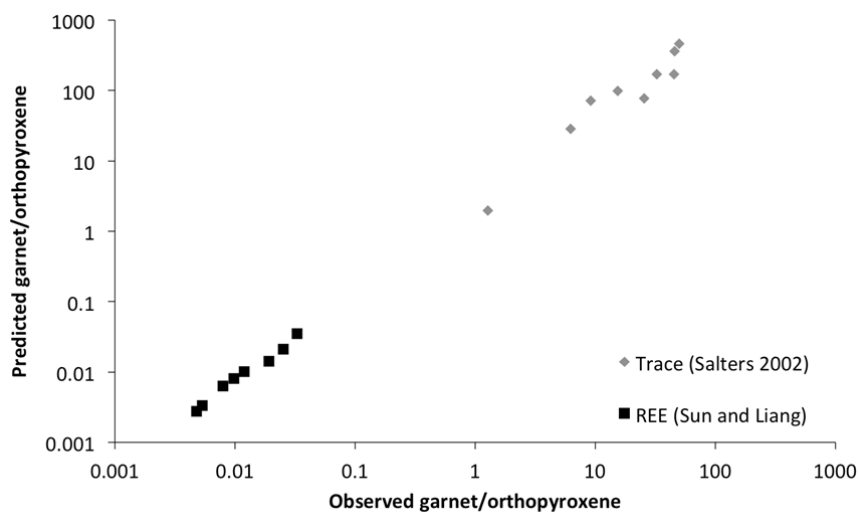


Figure DR2: Observed 'vs' predicted garnet/orthopyroxene ratios for the megacryst in BP002.

References

- Salters, V.J.M., Longhi, J.E. and Bizimis, M. (2002) Near mantle solidus trace element partitioning at pressures up to 3.4GPa. *Geochemistry, Geophysics, Geosystems*, 3, DOI:10.1029/2001GC000148.
- Sun, C. G. and Liang, Y. (2013) 'The importance of crystal chemistry on REE partitioning between mantle minerals (garnet, clinopyroxene, orthopyroxene, and olivine) and basaltic melts', *Chemical Geology*, 358, pp. 23-36.

Table DR1. Major and trace element data

wt%	Olivine		Garnet				Orthopyroxene			Precursor	
	Xenolith	2σ (n=9)	Xenolith	2σ (n=33)	Megacryst	2σ (n=21)	Xenolith	2σ (n=30)	Megacryst	2σ (N=26)	Megacryst
SiO ₂	41.59	0.59	42.41	0.23	41.73	0.71	58.15	0.21	58.38	0.49	56.65
Al ₂ O ₃	<LOD	-	21.26	0.27	21.91	0.89	0.75	0.07	0.74	0.06	2.94
Cr ₂ O ₃	<LOD	-	3.52	0.37	3.53	0.31	0.27	0.03	0.27	0.05	0.61
FeO	6.52	0.15	6.37	0.10	6.27	0.17	3.99	0.10	4.00	0.10	4.24
MnO	0.07	0.05	0.25	0.04	0.26	0.04	0.08	0.04	0.07	0.03	0.09
MgO	51.83	0.57	21.70	0.26	21.88	0.19	36.45	0.25	36.20	0.52	34.71
CaO	-	-	4.48	0.13	4.39	0.20	0.32	0.04	0.33	0.04	0.75
Mg#	93.4		85.9		86.2		94.20		94.1		93.60
Ts (%)	-		-		-		1.1		1.1		5.40
ppm				2σ (n=10)		2σ (n=7)		2σ (n=7)		2σ (n=6)	
Sc	-	-	94	13	87	9	2.6	1.2	2.4	0.3	11.25
V	-	-	200	30	176	15	43	10	37	3	51.2
Cr	-	-	-	-	-	-	2070	322	1978	1316	-
Mn	-	-	2478	177	2417	192	631	139	631	99	817
Co	-	-	41	5	42	5	50	10	50	5	49.2
Ni	-	-	40	6	39	3	801	123	766	206	691
Y	-	-	3.1	0.8	3.4	1.1	0.009	0.002	0.010	0.004	0.37
Zr	-	-	67	10	70	10	0.38	0.09	0.41	0.06	7.70
Nb	-	-	0.25	0.08	0.25	0.09	0.16	0.03	0.13	0.01	0.14
La	-	-	0.10	0.04	0.06	0.04	0.010	0.003	0.006	0.001	0.011
Ce	-	-	1.6	0.2	1.1	0.7	0.053	0.017	0.038	0.009	0.146
Pr	-	-	0.65	0.10	0.51	0.18	0.013	0.004	0.011	0.003	0.063
Nd	-	-	5.1	1.1	4.8	0.7	0.085	0.021	0.067	0.005	0.558
Sm	-	-	2.5	0.4	2.4	0.3	0.026	0.004	0.024	0.004	0.270
Eu	-	-	0.96	0.14	0.92	0.15	0.008	0.001	0.007	0.001	0.102
Gd	-	-	2.4	0.4	2.5	0.5	0.016	0.005	0.016	0.002	0.276
Dy	-	-	1.1	0.2	1.2	0.3	0.005	0.001	0.004	0.001	0.131
Ho	-	-	0.12	0.02	0.14	0.04	0.000	0.000	0.000	0.000	0.015
Er	-	-	0.21	0.05	0.22	0.07	<LOD	-	<LOD	-	-
Yb	-	-	0.15	0.02	0.15	0.03	<LOD	-	<LOD	-	-
Lu	-	-	0.03	0.01	0.03	0.01	<LOD	-	<LOD	-	-
Hf	-	-	0.91	0.16	0.97	0.11	0.013	0.006	0.013	0.003	0.113
Th	-	-	0.01	0.01	0.01	0.01	0.001	0.001	0.001	0.001	0.002
U	-	-	0.08	0.09	0.11	0.12	0.001	0.001	0.001	0.001	0.012

error is 2sd

P (GPa) reference

- 4.37 Brey, G.P. & Koehler, T. (1990). Geothermobarometry in four-phase lherzolites II. New thermobarometers, and practical assessment of existing thermobarometers. *Journal of Petrology* 31, 1353–1378.
- 4.12 Brey, G.P., Bulatov V.K. & Gurnis A.V. (2008). Geobarometry for Peridotites: Experiments in Simple and Natural Systems from 6 to 10 GPa. *Journal of petrology*, 49, 1460-2415
- 4.53 Nickel, K.G. & Green, D.H. (1985). Empirical geothermobarometry for garnet peridotites and implications for the nature of the lithosphere, kimberlites and diamonds. *Earth Planetary Science Letters* 73, 158–170.
- 4.50 MacGregor, I.D. (1974). The system MgO–Al₂O₃–SiO₂: solubility of Al₂O₃ in enstatite for spinel and garnet peridotite compositions. *American Mineralogist* 59, 110–119.
- 4.04 Ryan, C. G., Griffin, W. L. & Pearson, N. J. (1996). Garnet geotherms: pressure–temperature data from Cr-pyrope garnet xenocrysts in volcanic rocks. *Journal of Geophysical Research* 101, 5611–5625.